

An Infra-Red-Based Prototype for a Miniaturized Transcutaneous Carbon Dioxide Monitor

Tuna B. Tufan, Devdip Sen, and Ulkuhan Guler

Abstract—New types of miniaturized biomedical devices transform contemporary diagnostic and therapeutic techniques in medicine. This evolution has demonstrated exceptional promise in providing infrastructures for enabling precision health by creating diverse sensing modalities. To this end, this paper presents a prototype for transcutaneous carbon dioxide monitoring to diversify the measurable critical parameters for human health. Transcutaneous carbon dioxide monitoring is a noninvasive, surrogate method of assessing the partial pressure of carbon dioxide in the blood. The partial pressure of carbon dioxide is a vital index that can help understand momentarily changing ventilation trends. Therefore, it needs to be reported continuously to monitor the ventilatory status of critically ill patients. The proposed prototype employs an infrared LED as the excitation source. The infrared emission, which decreases in response to an increasing carbon dioxide concentration, is applied to a thermopile sensor that can detect the infrared intensity variations precisely. We have measured the changes in the partial pressure of carbon dioxide in the range of 0-120 mmHg, which covers humans' typical values, 35-45 mmHg. The prototype occupies an area of 25 cm² (50 mm×50 mm) and consumes 85 mW power.

I. INTRODUCTION

With the advent of sensing technologies and the miniaturization of devices in recent years, wearable biomedical sensors have become an integral part of the healthcare system. Next-generation biomedical devices like wearables can provide alternative measurement ways to bulky, wired, and obtrusive devices only used in clinical settings. New developments in next-generation biomedical device technologies bring healthcare to homes with wireless, remote and continuous monitoring of vital signs such as cardiac and respiratory parameters [1], [2].

Respiratory vital parameters are key indicators of the physiological status of the human body. The effectiveness of respiration action, inhaling in oxygen (O₂) and exhaling out carbon dioxide (CO₂), is measured by blood gases. The measurement of arterial blood gases (ABGs), namely, the partial pressure of oxygen (PaO₂), the partial pressure of carbon dioxide (PaCO₂), and the potential of hydrogen (pH), provide critical clinical information about the respiratory and metabolic condition of patients, such as arterial oxygenation, ventilation, and acid-base status [3]. More specifically, the diagnosis of diseases like acute respiratory distress syndrome (ARDS), chronic obstructive pulmonary disease (COPD), acute respiratory failure, heart failure, and asthma, is possible with blood gases information [4].

T.B. Tufan, D. Sen, and U. Guler are with the Department of Electrical and Computer Engineering, Worcester Polytechnic Institute, Worcester, MA 01609 USA.

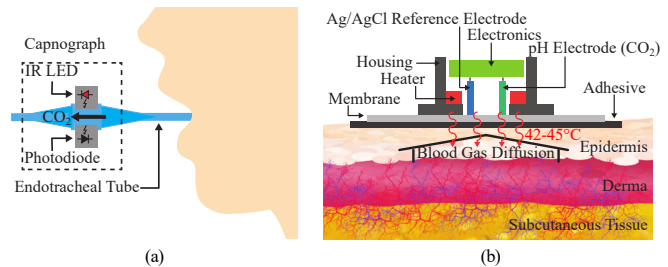


Fig. 1. Noninvasive methods for carbon dioxide monitoring [11]: a) capnography method, b) transcutaneous monitoring with electrochemical sensors.

While new blood gas monitoring devices and techniques are emerging [5]–[7], the need for a multimodal, wireless, and remote blood gas monitoring system has yet to be fulfilled. Particularly, efforts on miniaturization of transcutaneous CO₂ monitors are limited [8]. Among blood gases, PaCO₂ indicates the adequacy of alveolar ventilation as it is directly proportional to CO₂ extraction rate, which is inversely proportional to lung's alveolar ventilation [3]. A rise in PaCO₂ levels is compensated by increasing ventilation rate in healthy subjects. However, in cases including respiratory muscle fatigue, neuromuscular disorder, obstructive lung disease, obesity, or thoracic cage deformity, the ventilatory system can fail, leading to hypercapnia and hypocapnia complications, excessive and reduced CO₂ in the bloodstream, respectively [3]. Cardiac rhythm disorders, acute brain injury, and stroke are among the severe results of these complications [9].

The gold standard of assessing PaCO₂ is invasive ABG analysis, a painful procedure requiring a blood sample to be taken from the patient [4]. Other invasive methods alternative to ABG are arterialized capillary blood gas analysis (CBG) and peripheral venous blood gas analysis (VBG) [10]. These methods are also painful, break the skin integrity, and require a skilled professional. Additionally, all types of invasive blood gas analysis, giving only a brief and selective account of the ventilatory status, are not feasible for continuous monitoring.

The drawbacks of invasive blood gas analysis methods have led to a shift towards noninvasive methods, e.g., capnography and transcutaneous monitoring. While capnography monitors the partial pressure of CO₂ in the respiratory gases at the end of exhaled breath (PetCO₂), transcutaneous monitoring measures the partial pressure of CO₂ on the skin surface (PtcCO₂) [10], [12]–[15]. Capnography method relies on the infrared absorption of CO₂ in a specific wavelength [14], whereas current transcutaneous CO₂ monitors

utilize an electro-chemical measurement technique that deploys Severinghaus electrodes [16]. In this technique, the skin must be heated to obtain sufficient CO₂ diffusion [17], which can be obtrusive for the patients. Besides electro-chemical measurement based PtcCO₂ monitors, infra-red-based PtcCO₂ monitors have started to regain attention for medical use due to the need for a more stable and sensitive monitoring solution. [8], [18], [19]. Studies have shown that the estimation of PaCO₂ from PtcCO₂ can be done with a correlation coefficient as high as 0.89 [20].

In this paper, we present a prototype of a nondispersive infrared (NDIR) based transcutaneous carbon dioxide sensing system. Section II covers the related work in the field of transcutaneous carbon dioxide sensing and the motivation behind our efforts. In Section III, we explain the system architecture and the working principle of our prototype. Section IV demonstrates the measurement setup and presents the experimental results along with a performance comparison of recent designs in the literature and our work. Conclusion remarks are given in Section V.

II. PRIOR WORK AND MOTIVATION

Traditional transcutaneous CO₂ monitors sense changes in CO₂ diffusing through the skin with an electrochemical sensor. Dissolved CO₂ in the sensor solution alters the pH of the sensor electrolyte, creating a potential difference between the electrolyte-covered glass electrode and the Ag/AgCl reference electrode. The potential difference can be translated into the CO₂ concentration by using the Henderson-Hasselbalch equation [21]. Nevertheless, these traditional sensors are equipped with expensive, bulky bedside electronics; therefore, not suitable for continuous monitoring outside the clinical setting. Another disadvantage of electrochemical sensors is the requirement of frequent calibration due to the measurement drift over time, which impacts the sensor's reliability in the long-term. Moreover, the skin must be heated to 42°C or higher to obtain sufficient CO₂ diffusion and achieve accurate sensing. The heating requirement makes the sensing device obtrusive and increases power consumption drastically, which hinder the possibility of transforming it into a wearable device.

Another method of measuring CO₂ is with NDIR-based sensors that have been used in a wide range of applications such as air quality monitoring [22], and PetCO₂ monitoring for breath analysis [23]. The operation principle of NDIR systems is based on the Lambert and Beer law, which states that the IR radiation propagating through a gas medium attenuates in certain wavelengths specific to the absorption spectrum of the gas constituting the propagation medium [24]. The absorption wavelength for CO₂ is 4.26 μm.

With the prototype presented in this paper, our motivation is to create an accurate and sensitive transcutaneous carbon dioxide sensing device that can detect PtcCO₂ ranging from human's typical values (35-45 mmHg) to hypocapnia (<35 mmHg) and hypercapnia (>45 mmHg) levels. This prototype is the initial step towards a wearable NDIR-based transcutaneous carbon dioxide sensor.

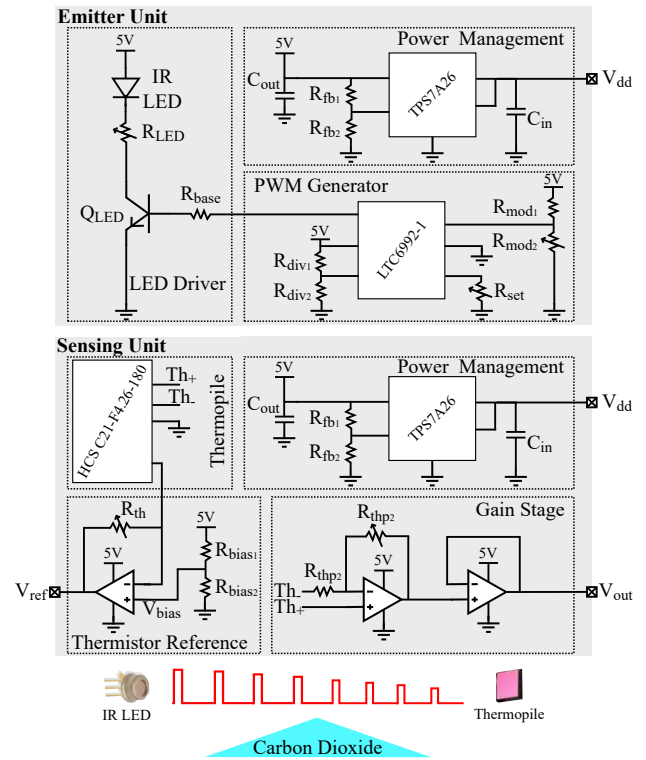


Fig. 2. Schematic diagram of the IR-based transcutaneous CO₂ monitor.

III. DESIGN AND METHODOLOGY

The proposed system, depicted in Fig.2, comprises an IR LED as an excitation source and a thermopile as a thermal sensing device. The CO₂ sensing mechanism relies on the fact that CO₂ has an absorption peak at 4.26 μm in the IR spectrum, hence making the thermopile output inversely proportional to the CO₂ concentration.

A. System Architecture

The prototype consists of two units; the emitter and sensing units, as demonstrated in Fig.2. Both units have a power management block, composed of a low-dropout (LDO) linear voltage regulator (TPS7A26, Texas Instruments, Dallas, TX) that provides a stable 5 V for the rest of the circuit. The emitter unit also includes a pulse width modulation (PWM) generator (LTC6992-1, Analog Devices, Wilmington, MA) with an adjustable duty cycle range of 0% to 100% and can be controlled by an external analog signal, an LED driver, and a mid-IR LED (L15895-0430M, Hamamatsu, Japan) with a peak emission wavelength of 4.26 μm corresponding to the peak absorption wavelength of CO₂.

The sensing unit, in addition to the power management block, comprises a thermopile sensor (HCS C21-F4.26-180, Heimann Sensor, Germany) with a built-in thermistor and a bandpass filter for sensing 4.26 μm wavelength, a gain stage to amplify the thermopile's output, and a thermistor reference block to calibrate the output of the built-in thermistor. Both PCB prototypes are 50 mm×50 mm.

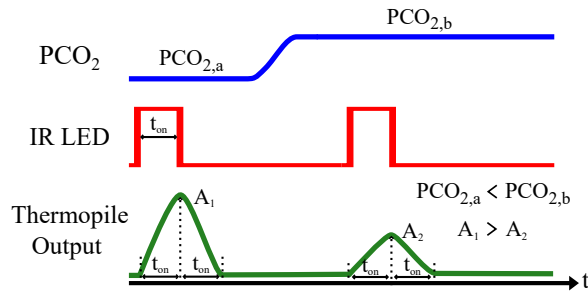


Fig. 3. Conceptual waveforms of IR-based CO₂ sensing with a pulsed LED.

B. Operation Principle

The PWM generator feeds the LED driver with a 5-Hz pulse. We opted to use this pulsing rate to capture changes in the CO₂ concentration considering getting enough samples in a respiration cycle and to avoid thermal drifts in the thermopile sensor. Therefore, the pulsing rate is high enough to follow a relatively slow signal, CO₂ concentration variation, and slow enough to provide the thermopile a sufficient cooldown time. We set the duty cycle of the pulse to 25% to reduce the power consumption. 25% duty cycle yields a good compromise between the power dissipation and the amount of IR radiation in each cycle that can provide input with enough precision to the thermopile. The LED driver is responsible for controlling the IR intensity. We adjust the intensity with the potentiometer in the LED driver block. IR LED radiates to the gas chamber with a peak emission wavelength of 4.26 μm .

The thermopile in the sensing unit converts the IR intensity information to a voltage value with temperature sensing thermocouples. The gain stage amplifies the thermopile output from μV range to the mV range. The amplified thermopile voltage, denoted as V_{out} in Fig.2, is the main output of the sensing unit where the CO₂ concentration is monitored. V_{ref} in Fig.2, denotes the output of thermistor reference block. The purpose of this block is to compensate for the ambient temperature changes. Fig.3 illustrates the relation between the output of the IR LED and the thermopile in the presence of a time-varying CO₂ concentration. As can be seen in Fig. 3, the amplitude of the thermopile's output is lower when the CO₂ concentration is higher since the IR absorption is proportional to the CO₂ concentration.

IV. MEASUREMENT RESULTS

The in vitro measurement setup, demonstrated in Fig.4, was built to test the performance of the proposed CO₂ monitor under varying partial pressure of CO₂ (PCO₂). An aluminum chamber was designed to be used as a measurement unit, we selected aluminum to have non-degrading high reflection surfaces inside the chamber. This avoids absorption of the IR radiation along the optical path and increases power efficiency. The emitter and sensor units were placed on the top and bottom sides of the chamber to the designated openings such that the IR LED and the thermopile are facing each other inward the chamber. Sapphire, a material significantly transparent to IR radiation (around 90% transmission

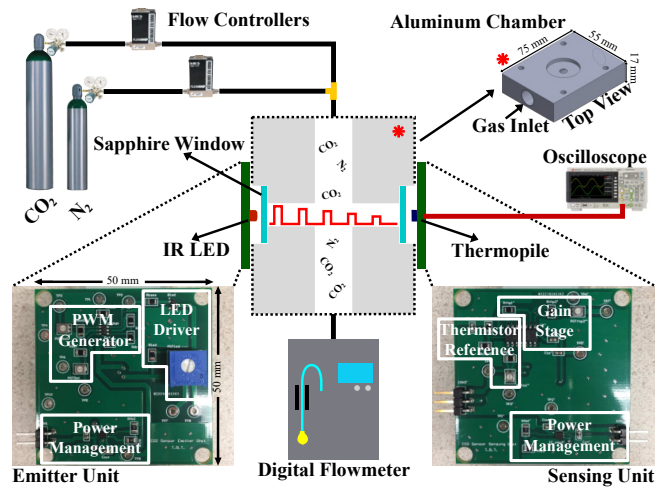


Fig. 4. In vitro measurement setup with the emitter and sensing PCBs.

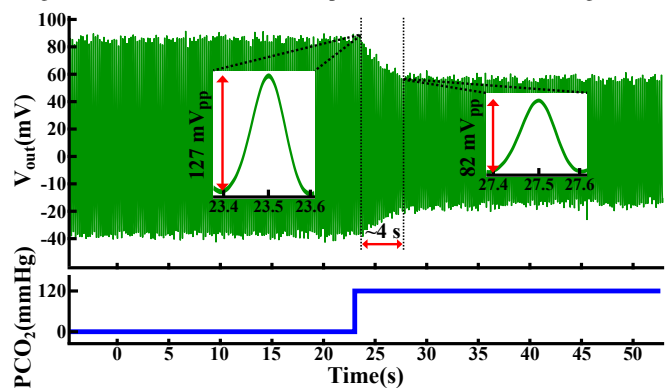


Fig. 5. The transient response of the sensing unit to a step change in PCO₂ from 0 mmHg to 120 mmHg.

at 4.26 μm), windows were utilized as a seal on both openings to avoid any gas leakage.

The PCO₂ inside the chamber was adjusted by mixing CO₂ with nitrogen (N₂) and setting the molar flow rate ratio ($\dot{M}_{CO_2}/\dot{M}_{N_2}$) of the gas mixture. We used two flow controllers for that purpose in between the gas cylinders and the chamber. The gas mixture was fed to the chamber through the gas inlet. We measured the flow rates with a digital flowmeter at the outlet of the chamber to ensure that the rates are set correctly.

In our first experiment, we observed the transient response of the CO₂ monitor to a step change in the PCO₂. We increased the PCO₂ in the measurement chamber from 0 mmHg to 120 mmHg and measured the sensing unit's output, V_{out} . As can be seen in Fig.5, the peak-to-peak voltage of the output drops to 82 mV_{pp} from 127 mV_{pp} in response to a 120 mmHg increase in the PCO₂. The measured response time is 4 s. In our second experiment, the output of the sensing unit was recorded for PCO₂ values ranging from 0 mmHg to 120 mmHg in steps of 15 mmHg. Fig.6 demonstrates the time-averaged shape of the sensing unit's output and the peak-to-peak value of the time-averaged output under varying PCO₂ levels. Before taking the time average, we filtered out the high frequency noise in the raw output signal, V_{out} . The time average was calculated over one period of the

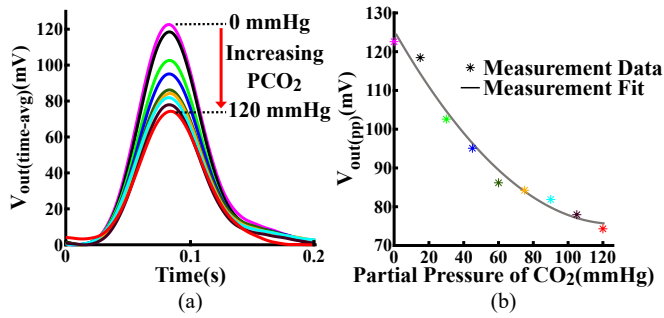


Fig. 6. a) Time-averaged output of the sensing unit and b) the peak-to-peak value of the time-averaged output for different PCO_2 levels.

TABLE I

COMPARISON OF PERFORMANCE PARAMETERS

Parameters	[19] 2005	[23] 2016	[18] 2020	This Work 2021
Sensor Type	Pyroelectric	Thermopile	Thermopile	Thermopile
Modality	PtcCO ₂	PetCO ₂	PtcCO ₂	PtcCO ₂
Power (mW)	NA	350	NA	85
Response time (s)	2	1.3	NA	~4
Range (mmHg)	1.52-15.2	0-38	30-50	0-120
Noise floor (mV _{RMS})	NA	NA	NA	30

output, which is 0.2 s. We observed the trend of decreasing sensor output with increasing PCO_2 up to 120 mmHg. We repeated the same experiment for different gain values by adjusting the gain stage in the sensing unit to evaluate the effect of the amplifier bandwidth on the sensing accuracy and we perceived the same trend in the sensor output. As the results evidence, the measurement range of the proposed CO_2 monitor covers the typical PCO_2 levels in humans (35-45 mmHg), also known as normocapnia, and the levels below (hypocapnia) and above (hypercapnia) the normocapnia that provide important clinical information.

Table 1 shows the performance parameters of the proposed CO_2 monitor and the relevant work in the literature. Our prototype consumes 85 mW which is significantly lower than the power consumption of the NDIR-based breath analyzer, 350 mW, proposed in [23]. The response time of our design and the works presented in [19], [23] are in a few seconds range and comparable. Our prototype can detect PCO_2 variation in a larger range, 0-120 mmHg, when compared to the measurement ranges of other reported works. The measured noise floor of our design is 30 mV_{RMS}.

V. CONCLUSION

In this work, we have proposed a miniaturized prototype that has the potential of being used as a transcutaneous CO_2 wearable device for healthcare applications. The prototype based on an IR LED and thermopile reading circuits employed in the PtcCO₂ monitor. We have presented the in vitro measurement results that demonstrate the successful monitoring of PCO_2 in 0-120 mmHg range which includes humans' typical values, 35-45 mmHg. The results also suggest that the detection of critical conditions such as hypocapnia and hypercapnia is possible with the proposed prototype.

REFERENCES

- [1] Y. A. Bhagat *et al.*, "Like Kleenex for Wearables: A soft, strong and disposable ECG monitoring system," in *2018 IEEE Biomedical Circuits and Systems Conference (BioCAS)*, Oct. 2018, pp. 1-1.
- [2] H. U. Chung *et al.*, "Binodal, wireless epidermal electronic systems with in-sensor analytics for neonatal intensive care," *Science*, vol. 363, no. 6430, Mar. 2019.
- [3] E. P. Trulock, "Arterial Blood Gases," in *Clinical Methods: The History, Physical, and Laboratory Examinations*, 3rd ed., H. K. Walker *et al.*, Eds. Boston: Butterworths, 1990.
- [4] L. Gattinoni *et al.*, "Understanding blood gas analysis," *Intensive Care Medicine*, vol. 44, no. 1, pp. 91-93, Jan. 2018.
- [5] U. Guler *et al.*, "Emerging Blood Gas Monitors: How They Can Help With COVID-19," *IEEE Solid-State Circuits Magazine*, vol. 12, no. 4, 2020.
- [6] I. Costanzo *et al.*, "Fluorescent Intensity and Decay Measurement of Pt-Porphyrin Film for Determining the Sensitivity of Transcutaneous Oxygen Sensor," in *IEEE International Circuits and Systems Conference, (ISCAS)*, May 2020.
- [7] I. Costanzo *et al.*, "An Integrated Readout Circuit for a Transcutaneous Oxygen Sensing Wearable Device," in *IEEE Custom Integrated Circuits Conference, (CICC)*, March 2020.
- [8] P. Grangeat *et al.*, "First Evaluation of a Transcutaneous Carbon Dioxide Monitoring Wristband Device during a Cardiopulmonary Exercise Test*," in *2019 41st Annual International Conference of the IEEE Engineering in Medicine and Biology Society (EMBC)*, Jul. 2019.
- [9] G. F. Curley *et al.*, "Hypocapnia and Hypercapnia," in *Murray and Nadel's Textbook of Respiratory Medicine*. Elsevier, 2016, pp. 1527-1546.e8.
- [10] S. E. Huttman *et al.*, "Techniques for the Measurement and Monitoring of Carbon Dioxide in the Blood," *Annals of the American Thoracic Society*, vol. 11, no. 4, Apr. 2014.
- [11] I. M. Costanzo *et al.*, "Respiratory Monitoring: Current State of the Art and Future Roads," *IEEE Reviews in Biomedical Engineering*, pp. 1-1, 2020, conference Name: IEEE Reviews in Biomedical Engineering.
- [12] H.-J. Lin *et al.*, "End-tidal carbon dioxide measurement in preterm infants with low birth weight," *PLOS ONE*, vol. 12, no. 10, Oct. 2017.
- [13] I. Costanzo *et al.*, "A Prototype Towards a Transcutaneous Oxygen Sensing Wearable," in *IEEE Biomedical Circuits and Systems Conference, (BIOCAS)*, October 2019, pp. 1-4.
- [14] B. S. Nassar and G. A. Schmidt, "Estimating Arterial Partial Pressure of Carbon Dioxide in Ventilated Patients: How Valid Are Surrogate Measures?" *Annals of the American Thoracic Society*, vol. 14, no. 6, pp. 1005-1014, Jun. 2017.
- [15] M. Ochiai *et al.*, "Transcutaneous blood gas monitoring among neonatal intensive care units in Japan," *Pediatrics International*, vol. 62, no. 2, 2020.
- [16] J. Lunn and W. Mapleson, "The severinghaus pco₂ electrode: A theoretical and experimental assessment," *British Journal of Anaesthesia*, vol. 35, no. 11, pp. 666-678, Nov. 1963.
- [17] N. Herrell *et al.*, "Optimal temperature for the measurement of transcutaneous carbon dioxide tension in the neonate," *The Journal of Pediatrics*, vol. 97, no. 1, pp. 114-117, Jul. 1980.
- [18] P. Grangeat *et al.*, "Evaluation in Healthy Subjects of a Transcutaneous Carbon Dioxide Monitoring Wristband during Hypo and Hypercapnia Conditions*," in *2020 42nd Annual International Conference of the IEEE Engineering in Medicine Biology Society (EMBC)*, Jul. 2020.
- [19] D. E. Kim *et al.*, "Noninvasive Optical Transcutaneous pCO₂ Gas Sensor," *Sensors and Materials*, vol. 17, no. 5, p. 9, 2005.
- [20] M. Dicembrino *et al.*, "End-tidal CO₂ and transcutaneous CO₂: Are we ready to replace arterial CO₂ in awake children?" *Pediatric Pulmonology*, vol. 56, no. 2, 2021.
- [21] M. Sinclair *et al.*, "The use of the henderson-hasselbalch equation in routine medical practice," *Clin Chim Acta*, vol. 19, no. 1, Jan. 1968.
- [22] Jongwon Kwon *et al.*, "A study on NDIR-based CO₂ sensor to apply remote air quality monitoring system," in *2009 ICCAS-SICE*, Aug. 2009, pp. 1683-1687.
- [23] T. Vincent and J. Gardner, "A low cost MEMS based NDIR system for the monitoring of carbon dioxide in breath analysis at ppm levels," *Sensors and Actuators B: Chemical*, vol. 236, pp. 954-964, Nov. 2016.
- [24] D. F. Swinehart, "The beer-lambert law," *Journal of chemical education*, vol. 39, no. 7, p. 333, 1962.